Food therapy of scutellarein ameliorates pirarubicin-induced cardiotoxicity in rats by inhibiting apoptosis and ferroptosis through regulation of NOX2-induced oxidative stress

YING LAN[1*], FENGSHUN TIAN[2*], HENG TANG[1*], PENG PU[1], QUAN HE[1] and LIANG DUAN[3]

Departments of [1]Cardiology, [2]Endocrine and [3]General Practice,
The First Affiliated Hospital of Chongqing Medical University, Chongqing 400042, P.R. China

Received October 16, 2023; Accepted March 6, 2024

DOI: 10.3892/mmr.2024.13208

Abstract. Pirarubicin (THP) is one of the most commonly used antineoplastic drugs in clinical practice. However, its clinical application is limited due to its toxic and heart-related side effects. It has been reported that oxidative stress, inflammation and apoptosis are closely associated with cardiotoxicity caused by pirarubicin (CTP). Additionally, it has also been reported that scutellarein (Sc) exerts anti-inflammatory, antioxidant, cardio-cerebral vascular protective and anti-apoptotic properties. Therefore, the present study aimed to investigate the effect of food therapy with Sc on CTP and its underlying molecular mechanism using echocardiography, immunofluorescence, western blot, ROS staining, and TUNEL staining. The *in vivo* results demonstrated that THP was associated with cardiotoxicity. Additionally, abnormal changes in the expression of indicators associated with oxidative stress, ferroptosis and apoptosis were observed, which were restored by Sc. Therefore, it was hypothesized that CTP could be associated with oxidative stress, ferroptosis and apoptosis. Furthermore, the *in vitro* experiments showed that Sc and the NADPH oxidase 2 (NOX2) inhibitor, GSK2795039 (GSK), upregulated glutathione peroxidase 4 (GPX4) and inhibited THP-induced oxidative stress, apoptosis and ferroptosis. However, cell treatment with the ferroptosis inhibitor, ferrostatin-1, or inducer, erastin, could not significantly reduce or promote, respectively, the expression of NOX2. However, GSK significantly affected ferroptosis and GPX4 expression. Overall, the results of the present study indicated that food therapy with Sc ameliorated CTP via inhibition of apoptosis and ferroptosis through regulation of NOX2-induced oxidative stress, thus suggesting that Sc may be a potential therapeutic drug against CTP.

Correspondence to: Dr Quan He, Department of Cardiology, The First Affiliated Hospital of Chongqing Medical University, 1 Youyi Road, Yuanjiagang, Yuzhong, Chongqing 400042, P.R. China
E-mail: hequan822@aliyun.com

Dr Liang Duan, Department of General Practice, The First Affiliated Hospital of Chongqing Medical University, 1 Youyi Road, Yuanjiagang, Yuzhong, Chongqing 400042, P.R. China
E-mail: dl2085704861@sina.com

*Contributed equally

Key words: scutellarein, pirarubicin, oxidative stress, apoptosis, ferroptosis, cardiotoxicity

Introduction

Currently, malignant tumors seriously endanger human life and health. Chemotherapy is considered as the most significant treatment strategy against cancer (1-4). Pirarubicin (THP) is a common chemotherapeutic drug used clinically. However, due to its cardiotoxicity, its clinical application remains limited (5-8).

It has been reported that cardiotoxicity caused by pirarubicin (CTP) is closely associated with the occurrence of oxidative stress in cardiomyocytes (9-11). Reactive oxygen species (ROS), the key intermediate of oxidative stress, plays a significant role in CTP (12,13). NADPH oxidases (NOXs), a major intracellular enzymatic source of ROS, are transmembrane complexes with electron-transferring ability that produce ROS (14,15). NOX2 is abundantly expressed in cardiomyocytes (16,17). A previous study demonstrated that increased ROS levels promoted mitochondrial dysfunction and it was therefore considered as a significant factor in mitochondria-mediated apoptosis (18). In addition, enhanced ROS levels have also been associated with lipid peroxidation, which in turn promotes the onset of a unique cell death mode, namely ferroptosis (19).

Scutellarein (Sc), a flavone monomer with known anti-inflammatory and antioxidant properties, is widely used in food and medical products (20-22). Previous studies demonstrated that Sc could improve oxidative stress in a diabetes mouse model and superoxide-induced rat cortical synaptosomes (23,24). Based on the aforementioned findings, it was hypothesized that food therapy with Sc ameliorated CTP via inhibition of apoptosis and ferroptosis through regulation of oxidative stress. However, this hypothesis has not been confirmed in *in vivo* or *in vitro* studies, while the effect of Sc on NOX2 remains largely unknown.

The present study aimed to explore the anti-oxidative stress, anti-ferroptosis and anti-apoptotic properties of Sc and the effects of the Sc-related key pathways on regulating oxidative stress, apoptosis and ferroptosis in CTP.

Materials and methods

Materials. The H9c2 cardiomyocyte cell line (cat. no. ZQ0102) was provided by Shanghai Zhongqiao Xinzhou Biotechnology Co., Ltd. THP, Sc, dexrazoxane (Dex; a drug particularly approved by the US Food and Drug Administration for the treatment of CTP), GSK2795039 (GSK), ferrostatin-1 (Fer-1) and erastin were purchased from MedChemExpress. The brain natriuretic peptide (BNP, cat. no. H166-1-2), creatine kinase MB (CK-MB, cat. no. H197-1-1) and cardiac troponin T (cTnT, cat. no. H149-4-2) kits were purchased from Nanjing Jiancheng Bioengineering Institute. Cell Counting Kit-8 (CCK-8), ROS (cat. no. S0033M) and TUNEL (cat. no. C10088) apoptosis assay kits were purchased from Beyotime Institute of Biotechnology. DMEM and FBS were obtained from Gibco (Thermo Fisher Scientific, Inc.) and BioAgrio, respectively. The reduced glutathione (GSH, cat. no. A006-2-1), glutathione peroxidase (GSH-Px, cat. no. A005-1-2), catalase (CAT, cat. no. A007-1-1), malondialdehyde (MDA, cat. no. A003-1-2), superoxide dismutase (SOD, cat. no. A001-3-2), lactate dehydrogenase (LDH, cat. no. A020-2-2) and total antioxidant capacity (T-AOC, cat. no. A015-2-1) assay kits were obtained from Nanjing Jiancheng Bioengineering Institute. An iron assay kit (, cat. no. ab83366) was purchased from Abcam, while the antibodies against glutathione peroxidase 4 (GPX4), NOX2, NOX4, erythroid 2-related factor 2 (NRF2), Bax, Bcl-2, GAPDH, caspase 3 and caspase 9 from Proteintech Group, Inc.

Animal studies

Animal model and diet. In the present study, a total of 50 male Sprague-Dawley (SD) rats (weight, 180-200 g) were obtained from the Experimental Animal Center of Chongqing Medical University. Rats were maintained under specific pathogen-free conditions at 23±2˚C, 55±5% relative humidity, a 12-h light/dark cycle and had free access to food and water. The rats were randomly divided into the following five groups (n=10 rats/group): i) The normal diet group (ND), where rats were fed standard chow and injected with an equal volume of normal saline via the tail vein, once a week for eight weeks; ii) the Sc group (Sc), where rats were fed with Sc feed (100 mg/kg) and injected with an equal volume of normal saline via the tail vein, once a week for eight weeks; iii) the THP group (THP), where rats were fed with standard chow, while 3 mg/kg THP was injected into the tail vein once a week for eight weeks (25); iv) the Sc + THP group (Sc + THP), were rats were fed with Sc feed (100 mg/kg) and 3 mg/kg THP was injected into the tail vein once a week for eight weeks; and v) the Dex + THP group (Dex + THP), where rats were fed with standard chow, while 3 mg/kg THP and 30 mg/kg Dex was injected into the tail vein and abdominal cavity, respectively, once a week for eight weeks. The survival of rats was recorded every day, while food consumption and rat weight were recorded once a week.

Echocardiography. The experiment was completed at week 8. Rats were first anesthetized by isoflurane inhalation (2% for induction and 2% for maintenance). Subsequently, after removing the chest hair of rats, the VIVID E95 and L8-18I-D probes (General Electric Company) were used to perform doppler echocardiography to measure ejection fraction (EF), fractional shortening (FS), left ventricular end-diastolic diameter (LVIDd) and left ventricular end-systolic diameter (LVIDs).

Sample collection, preparation and biochemical analysis. Following overnight fasting, rats were weighed and euthanized by cervical dislocation following anesthesia with 1% pentobarbital (40 mg/kg). Rat hearts were then removed, weighed and stored at -80˚C until further use. A part of the heart tissues was homogenized and the levels of iron, GSH, GSH-Px, MDA, SOD and T-AOC were immediately measured, according to the manufacturer's instructions. Within 2 h, blood samples were collected from the abdominal aorta and centrifuged at 900 x g for 30 min at room temperature. The supernatant was then stored at -80˚C. The serum levels of LDH, BNP, CK-MB and cTnT were directly determined using the corresponding kits.

Cell studies

Cell culture, treatment and grouping. H9c2 cells were cultured in DMEM supplemented with 10% (v/v) FBS in a humidified incubator with 95% air and 5% CO_2 at 37˚C. To establish an *in vitro* injury model, H9c2 cells were treated with 5 μmol/l THP for 24 h. Subsequently, to evaluate the association between oxidative stress, ferroptosis and apoptosis in CTP, the *in vitro* experiments were carried out into two parts. Therefore, cells were grouped as follows: a) Direction of oxidative stress, including i) the control (CON) group, where cells were cultured in DMEM; ii) the THP group (THP), where cells were treated with 5 μmol/l THP for 24 h; iii) the Sc + THP group (Sc + THP), where cells were pretreated with 100 μmol/l Sc for 1 h followed by treatment with 5 μmol/l THP for 24 h; iv) the GSK group (GSK), where cells were treated with 25 μmol/l GSK for 24 h (26); v) the GSK + THP group (GSK + THP), where cells were co-treated with 5 μmol/l THP and 25 μmol/l GSK for 24 h; and vi) the Sc + GSK + THP group (Sc + GSK + THP), where cells were pretreated with 100 μmol/l Sc for 1 h followed by co-treatment with 5 μmol/l THP and 25 μmol/l GSK for 24 h. b) Direction of ferroptosis, including i) the CON group (CON), where cells were cultured in DMEM; ii) the THP group (THP), where cells were treated with 5 μmol/l THP for 24 h; iii) the Sc + THP group (Sc + THP), where cells were pretreated with 100 μmol/l Sc for 1 h, followed by treatment with 5 μmol/l THP for 24 h; iv) the Fer-1 group, where cells were treated with 10 μmol/l Fer-1 for 24 h (27); v) the Fer-1 + THP group (Fer-1 + THP), where cells were co-treated with 10 μmol/l Fer-1 and 5 μmol/l THP for 24 h; vi) the erastin group (erastin), where cells were treated with 5 μmol/l erastin for 24 h (28); and the erastin + Sc group (erastin + Sc), where cells were pretreated with 100 μmol/l Sc for 1 h, followed by co-treatment with 5 μmol/l erastin for an additional 24 h.

Cell viability assay. H9c2 cells were seeded in 96-well plates at a density of $5x10^3$ cells/well for 12 h, prior to use. Following treatment, a CCK-8 assay kit was used to evaluate cell viability.

Briefly, cells in each well were supplemented with 10 μl CCK-8 reagent followed by incubation for 2 h. Subsequently, the absorbance in each well was measured at a wavelength of 450 nm using a single-wavelength microplate reader.

ROS staining. Cells were seeded into 24-well plates and after reaching 50-60% confluency, they were treated with the indicated compounds. Subsequently, cells were stained with DCFH-DA dye (37˚C, 20 min), provided by the ROS kit, according to the manufacturer's instructions (Beyotime Institute of Biotechnology). Cells were observed under a fluorescence microscope and the positive stained area was measured using ImageJ v1.53c software (National Institutes of Health).

Cell apoptosis. For cell apoptosis assessment, cells were seeded into 24-well plates and after reaching 50-60% confluency, the cells were treated as previously described. Subsequently, cell apoptosis was assessed using a TUNEL apoptosis assay kit, according to the manufacturer's instructions. Briefly, following fixing at room temperature for 30 min (Immunostaining fixative, Beyotime Institute of Biotechnology, cat. no. P0098), H9c2 cells were washed with ice-cold PBS and stained with DAPI (at room temperature for 5 min, Beyotime Institute of Biotechnology, cat. no. C1005) and TUNEL dyes (protected from light, at 37˚C for 60 min). After washing, fluorescent images were captured under a fluorescence microscope and analyzed using ImageJ v1.53c software.

Immunofluorescence staining. Cells were fixed with 4% formaldehyde (at room temperature for 15 min), washed with PBS and were then permeabilized with 0.2% Triton X-100 (at room temperature for 20 min). Following blocking with goat serum (cat. no. C0265; Beyotime Institute of Biotechnology) at room temperature for 30 min, the cells were first incubated at 4˚C, overnight with primary antibodies against NOX2 (cat. no. 19013-1-AP; 1:200; Proteintech Group, Inc.) and then with the corresponding secondary antibody [FITC-labeled goat anti-rabbit IgG (H+L); cat. no. A0562; 1:500; Beyotime Institute of Biotechnology] at room temperature for 90 min. Finally, the cell nuclei were stained with DAPI (at room temperature for 5 min) and images were captured under a fluorescence microscope.

Western blot analysis. The protein expression levels of GAPDH (cat. no. 10494-1-AP; 1:5,000), NOX2 (cat. no. 19013-1-AP; 1:1,000), NOX4 (cat. no. 14347-1-AP; 1:1,000), NRF2 (cat. no. 16396-1-AP; 1:2,000), GPX4 (cat. no. 30388-1-AP; 1:500), Bax (cat. no. 50599-2-Ig; 1:2,000), Bcl-2 (cat. no. 26593-1-AP; 1:500), cleaved and total caspase 3 (cat. no. 19677-1-AP; 1:500), and cleaved and total caspase 9 (cat. no. 10380-1-AP; 1:500) were detected by western blot analysis. Briefly, H9c2 cells or cardiac tissue were lysed in RIPA lysis buffer (Beyotime Institute of Biotechnology) with 1% (v/v) phenylmethylsulfonyl fluoride. Following centrifugation at 13,700 x g for 15 min at 4˚C, the supernatants were collected and then the protein concentration was measured using a BCA protein determination kit. An equal amount of protein extracts (30 μg) was separated by 12% SDS-PAGE and proteins were then transferred onto a PVDF membrane. Following blocking with 5% (w/v) skimmed milk (at room temperature for 2 h), the membrane was cut into strips according to the molecular weight of each target-protein. Subsequently, the membrane was first incubated with primary antibodies overnight at 4˚C and then with the corresponding horseradish peroxidase-conjugated secondary antibodies (cat. no. SA00001-2; Proteintech Group, Inc.; 1:5,000). The protein bands were visualized using an ECL reagent (Biosharp life sciences, cat. no. BL520B). GAPDH served as an internal control for protein loading and analysis. ChemiDoc™ XRS+ with Image Lab Software (BIO-RAD) was used for densitometry.

Statistical analysis. GraphPad Prism 8.0 (Dotmatics) was used for statistical analysis. All experiments were repeated at least three times. The data are expressed as the mean ± standard deviation. First, the normal distribution and homogeneity of variance of the data were assessed. The differences between groups were compared using one- or two-way ANOVA, followed by Tukey's multiple comparison post hoc test. $P<0.05$ was considered to indicate a statistically significant difference.

Results

Sc effectively improves the THP-mediated changes in food intake, body weight, heart indexes and survival in SD rats. As shown in Fig. 1, compared with the ND group, food intake was significantly reduced from the third week in the THP group (THP vs. ND, $P<0.01$; Fig. 1B). In addition, rat weight was also notably decreased in the THP group at the fourth week compared with the ND group (THP vs. ND, $P<0.01$; Fig. 1A). After eight weeks, the survival rate of rats in the THP group was markedly reduced compared with the ND group (Fig. 1C), while the cardiac mass index was notably enhanced (THP vs. ND, $P<0.01$; Fig. 1D). However, co-treatment of rats with Sc and Dex significantly restored the aforementioned changes (Sc + THP vs. THP: $P<0.05$, cardiac mass index and $P<0.01$, body weight and food intake; Dex + THP vs. THP: $P<0.05$, cardiac mass index and $P<0.01$, body weight and food intake; Fig. 1A-D).

Sc effectively improves the THP-induced abnormal changes in myocardial injury markers and echocardiography in SD rats. As shown in Fig. 2, after treatment of SD rats with THP for eight weeks, significant changes were observed in the echocardiography parameters in the THP group compared with the ND group (Fig. 2A), including decreased EF and FS (THP vs. ND, $P<0.01$; Fig. 2B and C) and increased LVIDd and LVIDs (THP vs. ND, $P<0.01$; Fig. 2D and E). At the same time, abnormal levels of the myocardial injury-related markers, BNP, CK-MB, cTnT and LDH, were recorded in the THP group (THP vs. ND, $P<0.01$; Fig. 2F-I). However, the aforementioned changes were improved following treatment of SD rats with Sc and Dex (Sc + THP vs. THP, $P<0.05$ for FS, LVIDd, LVIDs, cTnT and LDH, and $P<0.01$ for EF, BNP, CK-MB; Dex + THP vs. THP, $P<0.05$ for EF, FS, LVIDd, LVIDs, BNP and LDH, and $P<0.01$ for CK-MB and cTnT; Fig. 2A-I).

Sc alleviates the THP-induced abnormal changes in the oxidative stress- and ferroptosis-related indexes in blood and myocardial tissues of SD rats. Compared with the ND

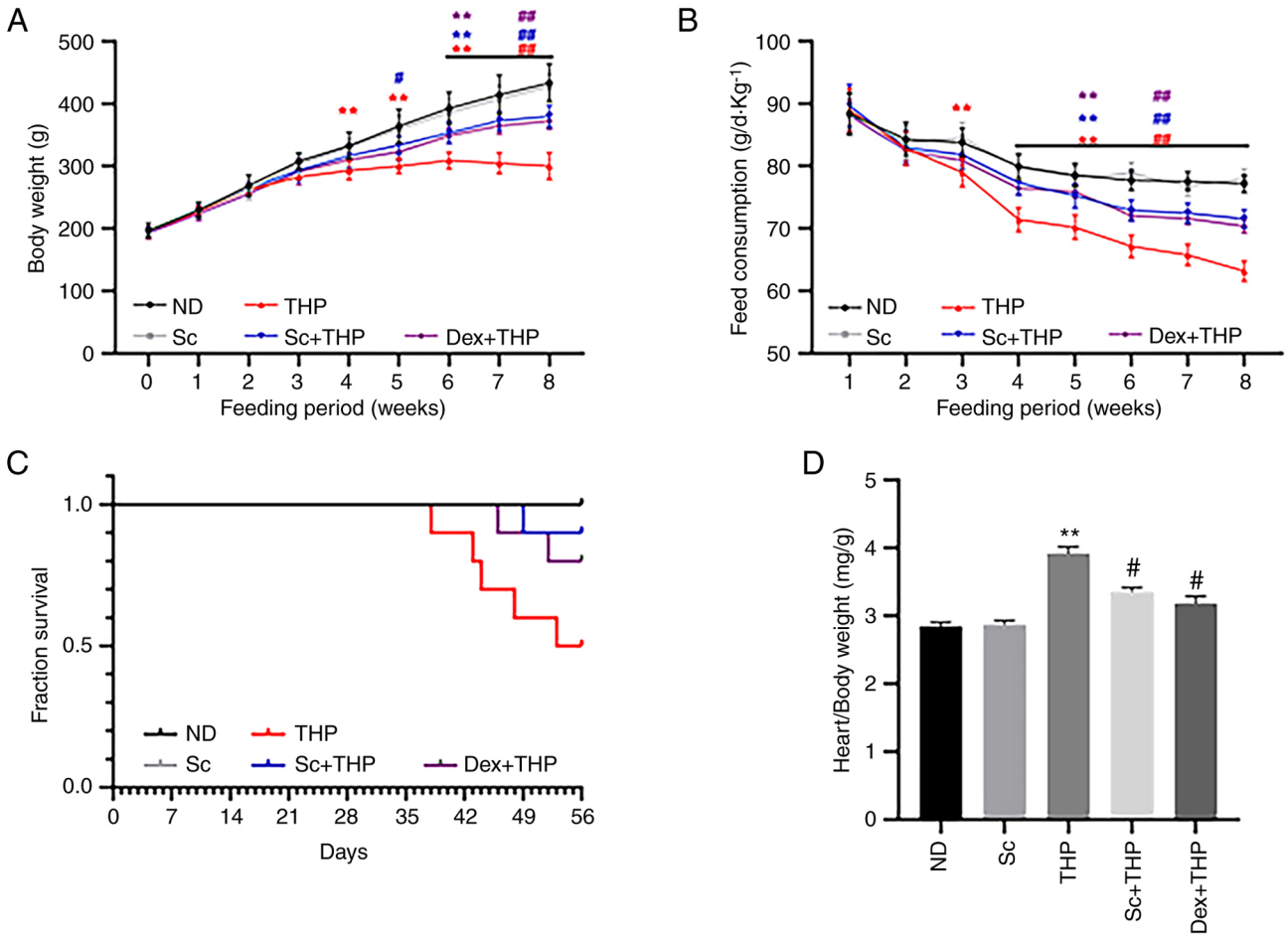

Figure 1. Sc improves the effects of THP on body weight, food intake, survival rate and heart/body weight of SD rats. Quantitative analysis of (A) body weight, (B) feed consumption, (C) fraction survival and (D) heart/body weight in each group. Values are expressed as the means ± standard deviation. **P<0.01 vs. CON. $^{\#}$P<0.05 and $^{\#\#}$P<0.01 vs. THP. THP, pirarubicin; CON, control; ND, normal diet; Sc, scutellarein; Dex, dexrazoxane.

group, Fe^{2+}, Fe^{3+} and total Fe levels were enhanced in the THP group (THP vs. ND, P<0.05 for Fe^{3+} and P<0.01 for Fe^{2+} and total Fe; Fig. 3A-C), while this effect was restored by rat treatment with Sc and Dex (Sc + THP vs. THP, P<0.05 for Fe^{2+} and total Fe; Dex + THP vs. THP, P<0.05 for Fe^{2+} and total Fe; Fig. 3A and C). In addition, the levels of CAT, GSH, GSH-Px, SOD and T-AOC were reduced (THP vs. ND, P<0.01; Fig. 3D-H), while the level of MDA was increased (THP vs. ND, P<0.01; Fig. 3I) in the THP group compared with the ND group, and these effects were also restored following treatment of SD rats with Sc and Dex (Sc + THP vs. THP, P<0.05 for CAT, GSH and SOD, and P<0.01for GSH-Px, T-AOC and MDA; Dex + THP vs. THP, P<0.05 for GSH, SOD and T-AOC, and P<0.01 for CAT, GSH-Px and MDA; Fig. 3D-I).

Effects of Sc and THP on the expression of oxidative stress-, ferroptosis- and apoptosis-related proteins in the myocardium of SD rats. The results of western blot analysis showed that THP increased the expression of oxidative stress-related proteins, such as NOX2 and NOX4, and decreased those of NRF2, in the myocardial tissues of SD rats (THP vs. ND, P<0.01 for NOX2 and NRF2, and P<0.001 for NOX4; Fig. 4A-D). Additionally, THP downregulated GPX4, a ferroptosis-related protein (THP vs. ND, P<0.01; Fig. 4E). In terms of apoptosis, THP notably enhanced the Bax/Bcl-2 ratio, the cleaved caspase 3/total caspase 3 and cleaved caspase 9/total caspase 9 ratio (THP vs. ND, P<0.001 for Bax/Bcl-2, cleaved caspase 3/total caspase 3 and cleaved caspase 9/total caspase 9; Fig. 4A and F-H), while these were restored by Sc and Dex (Sc + THP vs. THP, P<0.05 for NOX2, NRF2, GPX4, cleaved caspase 3/total caspase 3 and cleaved caspase 9/total caspase 9, and P<0.01 for NOX4, Bax/Bcl-2; Dex + THP vs. THP, P<0.05 for NOX2, NRF2, GPX4, Bax/Bcl-2, cleaved caspase 3/total caspase 3 and cleaved caspase 9/total caspase 9, and P<0.01 for NOX4; Fig. 4B-H).

Sc ameliorates the THP-mediated decrease in H9c2 myocardial cell viability. In vitro experiments using CCK-8 assays, showed that 5 μmol/l THP and 100 μmol/l Sc were the optimal concentrations to treat cells (5 μmol/l THP vs. CON, P<0.001; 100 μmol/l Sc + THP vs. THP, P<0.01; Fig. 5A and B). CCK-8 assays showed that THP significantly reduced the viability of H9c2 cells, which was improved by cell treatment with Sc, GSK and Fer-1 (THP vs. CON, P<0.01; Sc + THP vs. THP, P<0.05; GSK + THP vs. THP, P<0.05; and Fer-1 + THP vs. THP, P<0.05; Fig. 5C-E). Furthermore, erastin had a similar effect with THP on cell viability, which was also alleviated by Sc (erastin vs. CON, P<0.01; and erastin + Sc vs. erastin, P<0.01; Fig. 5E).

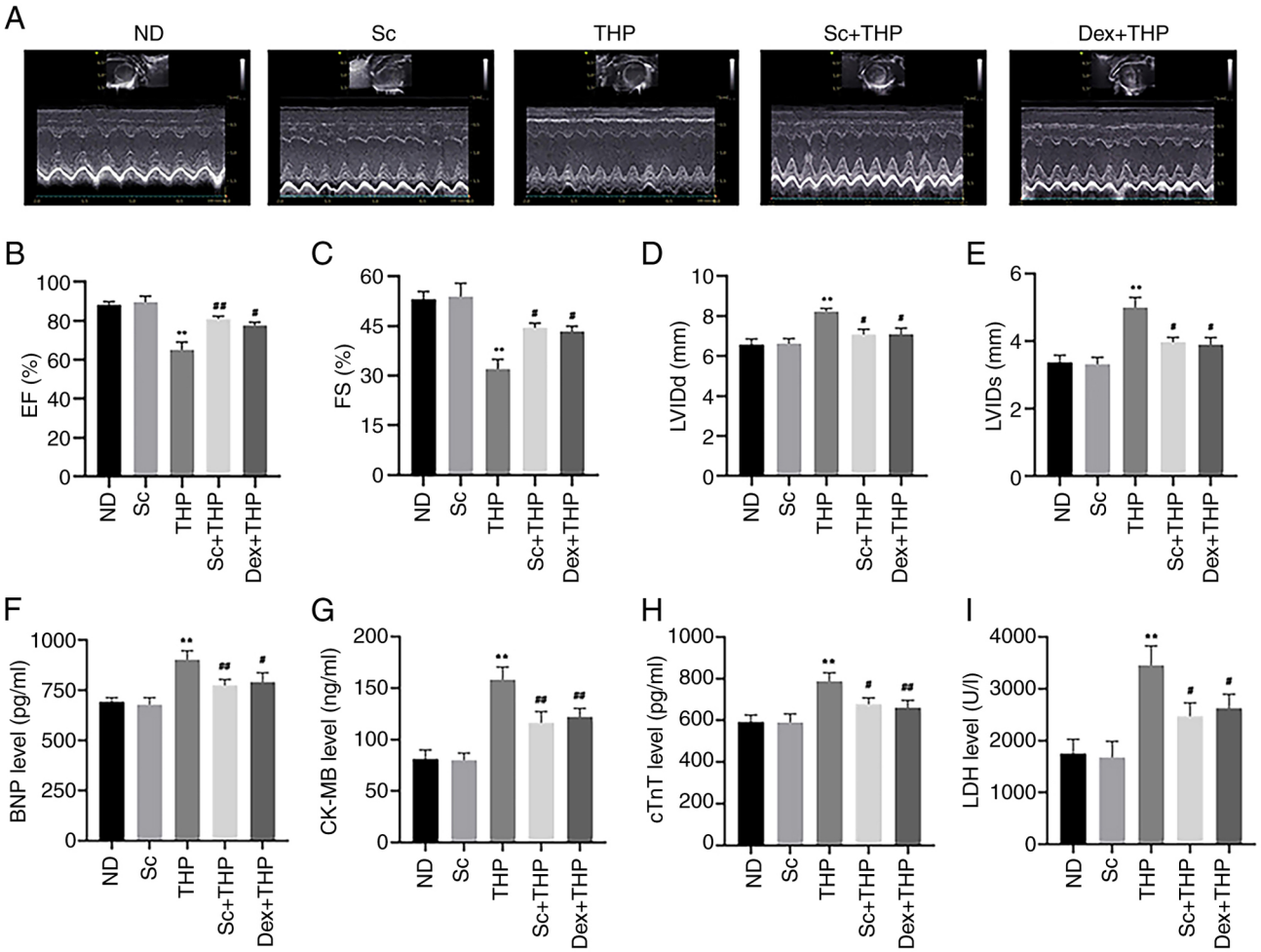

Figure 2. Sc improves the effects of myocardial injury markers and echocardiography results, induced by THP in SD rats. (A) Results of echocardiography in various groups. Quantitative analysis of the (B) EF, (C) FS, (D) LVIDd and (E) LVIDs in each group. Quantitative analysis in each group of the myocardial injury markers: (F) BNP, (G) CK-MB, (H) cTnT and (I) LDH. Values are expressed as the means ± standard deviation. **P<0.01 vs. CON. $^{\#}$P<0.05 and $^{\#\#}$P<0.01 vs. THP. Sc, scutellarein; THP, pirarubicin; EF, ejection fraction; FS, fractional shortening; LVIDd, left ventricular end-diastolic diameter; LVIDs, left ventricular end-systolic diameter; BNP, brain natriuretic peptide; CK-MB, creatine kinase MB; cTnT, cardiac troponin T; LDH, lactate dehydrogenase; ND, normal diet; Dex, dexrazoxane.

Effects of Sc, THP, GSK, Fer-1 and erastin on ROS generation in H9c2 cardiomyocytes. As shown in Fig. 5D and F, THP enhanced ROS production in H9c2 cells, while Sc and GSK antagonized this effect (THP vs. CON, P<0.01; Sc + THP vs. THP, P<0.01; and GSK + THP vs. THP, P<0.01; Fig. 5F). Furthermore, erastin also increased ROS production in H9c2 cells, which was alleviated by Sc (erastin vs. CON, P<0.01; erastin + Sc vs. erastin, P<0.01; Fig. 5F). Consistently, Fer-1 also improved the THP-mediated increase in ROS production (Fer-1 + THP vs. THP, P<0.01; Fig. 5F).

Effects of Sc, THP, GSK, Fer-1 and erastin on H9c2 cardiomyocyte apoptosis. TUNEL staining results indicated that THP promoted H9c2 cell apoptosis (THP vs. CON, P<0.01; Fig. 6A and B). This effect was abrogated by cell treatment with GSK, Fer-1 and Sc (Sc + THP vs. THP, P<0.01; GSK + THP vs. THP, P<0.01; and Fer-1 + THP vs. THP, P<0.01; Fig. 6A and B). In addition, erastin also enhanced H9c2 cell apoptosis, which was also improved by Sc (erastin vs. CON, P<0.01; erastin + Sc vs. erastin, P<0.01; Fig. 6A and B).

Effects of Sc, THP, GSK, Fer-1 and erastin on the expression of oxidative stress-, ferroptosis- and apoptosis-related proteins in H9c2 cardiomyocytes. The in vitro immunofluorescence results shown in Fig. 6C and D, revealed that compared with the CON group, NOX2 was upregulated in the THP group (THP vs. CON, P<0.01; Fig. 6C and D). The protein expression levels of NOX2 were restored following cell treatment with Sc and GSK (Sc + THP vs. THP, P<0.01; and GSK + THP vs. THP, P<0.01; Fig. 6C and D). However, Fer-1 and erastin did not significantly affect NOX2 expression. Furthermore, the western blot results also demonstrated that THP markedly upregulated NOX2, increased the Bax/Bcl-2, cleaved caspase 3/total caspase 3, cleaved caspase 9/total caspase 9 ratio and downregulated GPX4 (THP vs. CON, P<0.01 for cleaved caspase 3/total caspase 3; P<0.001 for GPX4, cleaved caspase 9/total caspase 9; and P<0.0001 for NOX2 and Bax/Bcl-2; Fig. 7C). The aforementioned results were restored by cell treatment with Sc (Sc + THP vs. THP, P<0.05 for NOX2, GPX4, Bax/Bcl-2, cleaved caspase 3/total caspase 3 and cleaved caspase 9/total caspase 9; Fig. 7C). At the same time, the aforementioned effects were also improved

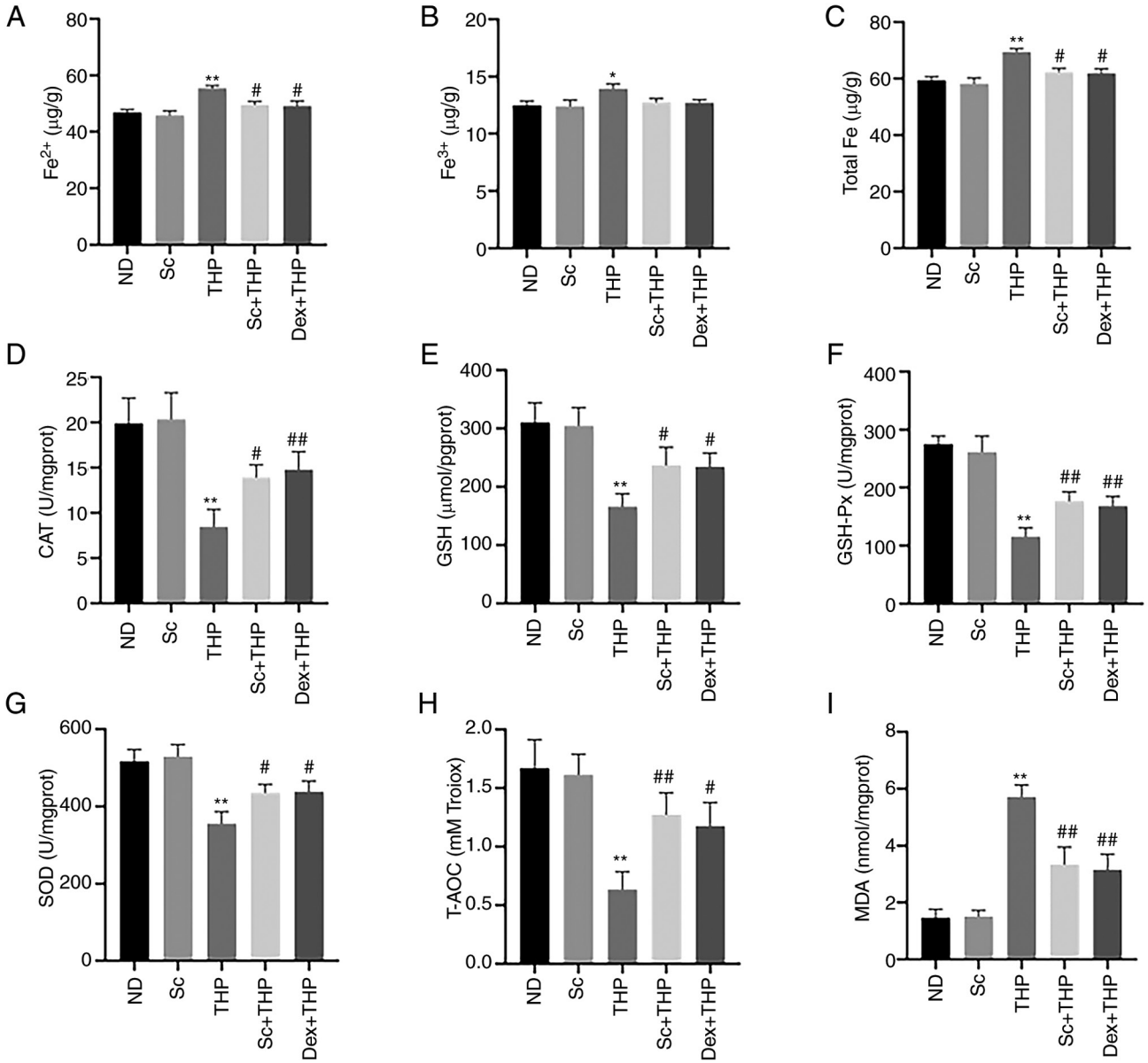

Figure 3. Sc alleviates the THP-induced aberrant effects of indexes related to oxidative stress and ferroptosis in blood and myocardial tissue *in vivo*. Quantitative analysis in each group of the indexes related to oxidative stress and ferroptosis: (A) Fe^{2+}, (B) Fe^{3+}, (C) total Fe, (D) CAT, (E) GSH, (F) GSH-Px, (G) SOD, (H) T-AOC, and (I) MDA. Values are expressed as the means ± standard deviation. *P<0.05 and **P<0.01 vs. CON. $^{\#}$P<0.05 and $^{\#\#}$P<0.01 vs. THP. Sc, scutellarein; THP, pirarubicin; CAT, catalase; GSH, glutathione; GSH-Px, glutathione peroxidase; SOD, superoxide dismutase; T-AOC, total antioxidant capacity; MDA, malondialdehyde; ND, normal diet; Dex, dexrazoxane.

by GSK treatment (GSK + THP vs. THP, P<0.05 for NOX2, GPX4, Bax/Bcl-2, cleaved caspase 3/total caspase 3 and cleaved caspase 9/total caspase 9; Fig. 7C). Consistent with the immunofluorescence results, erastin and Fer-1 had no effect on NOX2 expression (Fig. 7D). Notably, H9c2 cell treatment with erastin increased the Bax/Bcl-2 ratio, upregulated cleaved caspase 3/9, total caspase 3/9 and downregulated GPX4 (erastin vs. CON, P<0.01 for cleaved caspase 3/total caspase 3, cleaved caspase 9/total caspase 9; and P<0.001 for GPX4 and Bax/Bcl-2; Fig. 7D), while Sc improved some aforementioned effects (erastin + Sc vs. erastin, P<0.05 for cleaved caspase 3/total caspase 3 and cleaved caspase 9/total caspase 9; and P<0.01 for GPX4 and Bax/Bcl-2; Fig. 7D). In addition, Fer-1 improved aberrant protein effects in H9c2 cells induced by THP (Fer-1 + THP vs. THP, P<0.05 for GPX4, cleaved caspase 3/total caspase 3 and cleaved caspase 9/total caspase 9; and P<0.01 for Bax/Bcl-2; Fig. 7D).

Discussion

With the increasing incidence of malignant tumors, chemotherapy-induced myocardial toxicity has become a public health problem that cannot be ignored. CTP is considered as a significant component of the aforementioned problem (29,30). It has been reported that oxidative stress and ROS, a key product of oxidative stress, are closely associated with the onset of CTP in myocardial cells (8). Therefore, regulating oxidative stress can be a significant entry point for the prevention and treatment of CTP (31). In the present study, the results demonstrated that THP notably inhibited the growth of SD

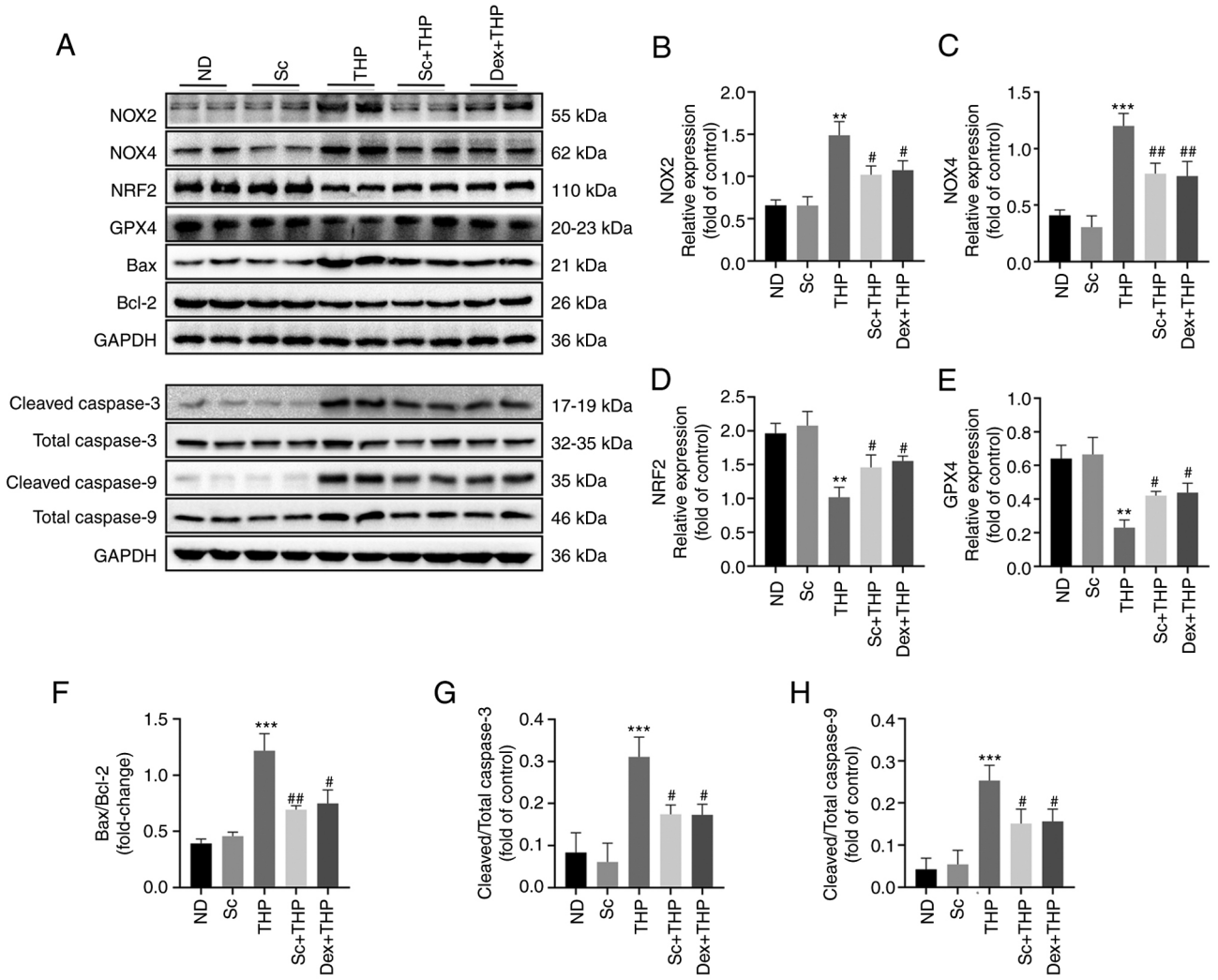

Figure 4. Sc improves the oxidative stress, ferroptosis, and apoptosis-related protein effects induced by THP in the myocardium of SD rats. (A) Western blots. Semi-quantitative analysis of the protein expression of (B) NOX2, (C) NOX4, (D) NRF2, (E) GPX4, (F) Bax/Bcl-2, (G) cleaved caspase 3/total caspase 3 and (H) cleaved caspase 9/total-caspase 9 in each group. Values are expressed as the means ± standard deviation. **P<0.01 and ***P<0.001 vs. ND. $^{\#}$P<0.05 and $^{\#\#}$P<0.01 vs. THP. Sc, scutellarein; THP, pirarubicin; NOX2, NADPH oxidase 2; NOX4, NADPH oxidase 4; NRF2, erythroid 2-related factor 2; GPX4, glutathione peroxidase 4; ND, normal diet; Dex, dexrazoxane.

rats, reduced their survival rate and severely impaired cardiac function, as verified by the abnormal elevation of the myocardial injury-related markers, BNP, CK-MB, cTnT and LDH, and the changes in cardiac echocardiography. The aforementioned findings verified that THP could successfully induce myocardial toxicity in SD rats. In addition, THP promoted abnormal changes in oxidative stress-related indexes in the blood and myocardium of SD rats, thus further supporting that oxidative stress may play a significant role in THP-induced myocardial toxicity. Notably, the *in vivo* experiments also revealed that THP promoted aberrant changes in the expression of apoptosis-related indicators, such as Bax, Bcl-2, cleaved caspase 3 and cleaved caspase 9, and ferroptosis-related indicators, including Fe^{2+}, total Fe and GPX4, in SD rats. Therefore, it was suggested that CTP may be associated with oxidative stress, ferroptosis and apoptosis.

Sc has strong antioxidant properties and is widely used in the medical and food industries (20-22). Therefore, herein, to explore the effect of Sc on CTP, SD rats were subjected to food therapy with Sc. Currently, oxidative stress is considered the central mechanism of anthracycline-induced myocardial toxicity (8,32). Different from other cells, myocardial cells have high energy demands and therefore are rich in mitochondria, where ROS-producing enzymes, such as NOX2, are located. Therefore, the majority of ROS is produced in mitochondria (33-35). When cells are induced, NOX2 is activated to produce ROS via delivering electrons from NADPH to oxygen through the transmembrane (36). Previous studies showed that anthracycline chemotherapeutic drugs aggravated oxidative stress in myocardial cells and promoted the production of ROS, thus suggesting that myocardial cells are vulnerable to anthracycline drugs (8,37). Consistent with the aforementioned finding, in the present study, treatment of myocardial cells with THP promoted oxidative stress and ROS overproduction. Furthermore, cell co-treatment with Sc improved the THP-mediated NOX2 upregulation, thus further improving the increase of ROS and alleviating the THP-induced oxidative stress.

Mitochondria are a significant regulatory target of apoptosis, while ROS is one of the triggering factors of mitochondrial-mediated apoptosis (38,39). Low levels of

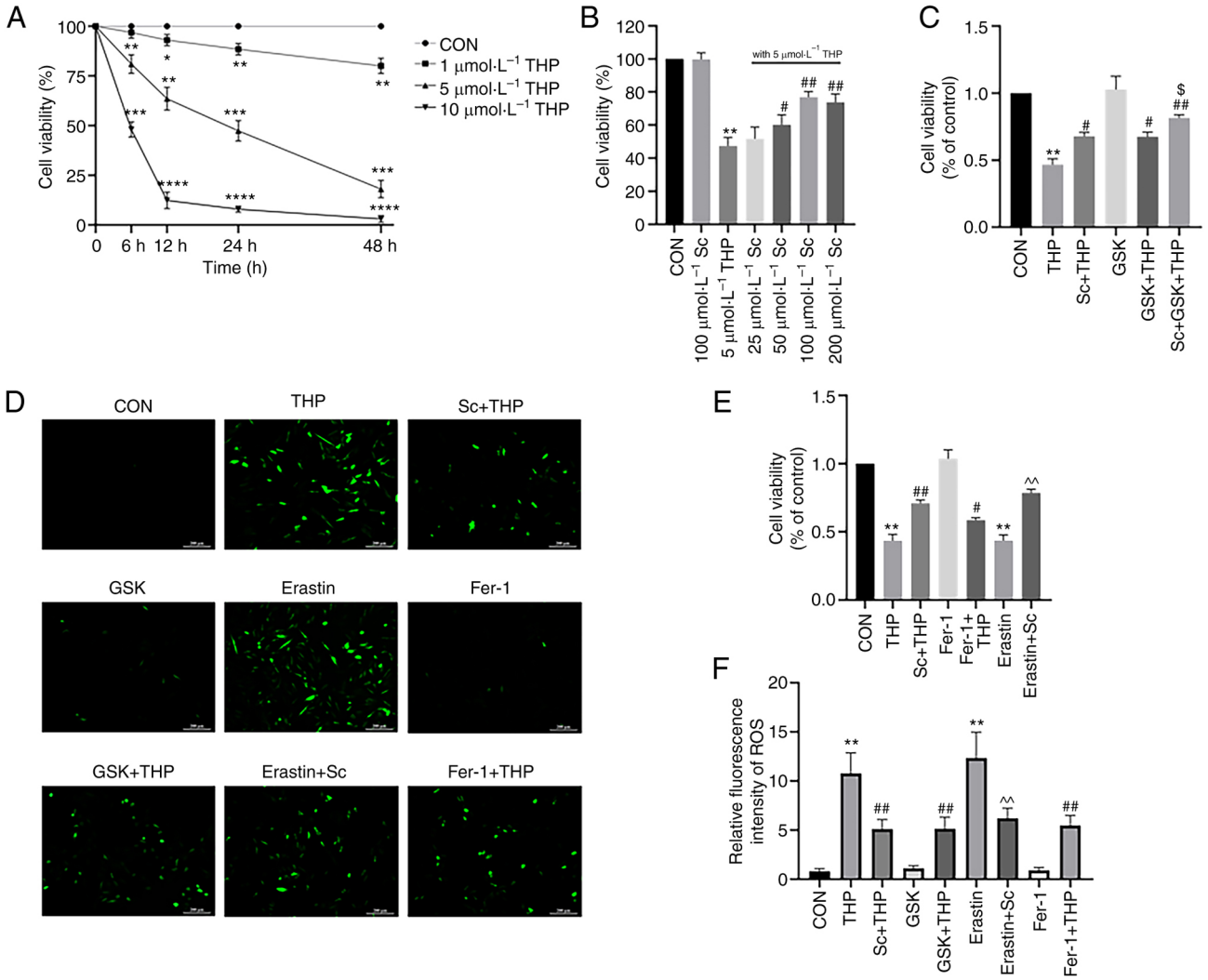

Figure 5. Effects of Sc, THP, GSK, Fer-1, and erastin on the cell viability and the production of ROS in H9c2 cells. According to CCK-8 assays, it was determined that the treatment concentration of THP was (A) 5 μmol/l and that of (B) Sc was 100 μmol/l. (C and E) Quantitative analysis of the CCK-8 assays in each group receiving corresponding treatment. (D) ROS staining. (F) Semi-quantitative analysis of ROS in each group. Values are expressed as the means ± standard deviation. *P<0.05, **P<0.01, ***P<0.001 and ****P<0.0001 vs. CON. $^{\#}$P<0.05 and $^{\#\#}$P<0.01 vs. THP. $^{\$}$P<0.05 vs. GSK + THP. $^{\wedge\wedge}$P<0.01 vs. erastin. Sc, scutellarein; THP, pirarubicin; GSK, GSK2795039; Fer-1, ferrostatin-1; ROS, reactive oxygen species; CCK-8, Cell Counting Kit-8; CON, control.

ROS are critical for cell proliferation, signal transduction and other physiological processes, while its enhanced levels are associated with cytotoxicity, which promotes DNA damage, mitochondrial dysfunction, reduced protein synthesis and destruction of intracellular calcium homeostasis, eventually leading to cardiomyocyte apoptosis (39-41). The results of the present study indicated that THP increased the expression of apoptosis-related proteins, namely Bax/Bcl-2, cleaved caspase 3 and cleaved caspase 9, in cardiomyocytes. However, treatment with Sc and GSK reversed these effects, thus suggesting that regulating oxidative stress could improve THP-induced cardiomyocyte apoptosis.

On the other hand, THP also promoted changes in the expression of the key ferroptosis-related protein, GPX4, thus supporting that in addition to oxidative stress and apoptosis, ferroptosis may be also involved in CTP. As aforementioned, THP induced oxidative stress and promoted ROS production in myocardial cells. A previous study showed that the excessive production of ROS induced lipid peroxidation, thus indicating that ferroptosis could be considered as a newly discovered unique method of cell death driven by iron-dependent lipid peroxidation (19). It has been reported that ferroptosis is regulated by several cellular metabolic pathways, such as iron homeostasis, redox homeostasis, mitochondrial activity and various disease-related signal transduction pathways (19,42,43). A previous study demonstrated that NOX4 promoted ferroptosis in astrocytes through oxidative stress-induced lipid peroxidation (44). GPX4, also known as phospholipid hydrogen glutathione peroxidase, prevented ferroptosis via converting lipid hydroperoxide into non-toxic lipid alcohols (42-44). Furthermore, astragaloside IV attenuated ferroptosis in myocardial cells via promoting the expression of GPX4 through activating the NRF2 signaling pathway and regulating oxidative stress (45).

In the present study, ferroptosis was induced and inhibited following cell treatment with erastin and Fer-1, respectively. Erastin is a ferroptosis inducer, which functions through ROS and iron-dependent signaling (46,47). A previous study showed that erastin inhibited voltage-dependent anion channels 2/3 and accelerated oxidation, thus leading to the

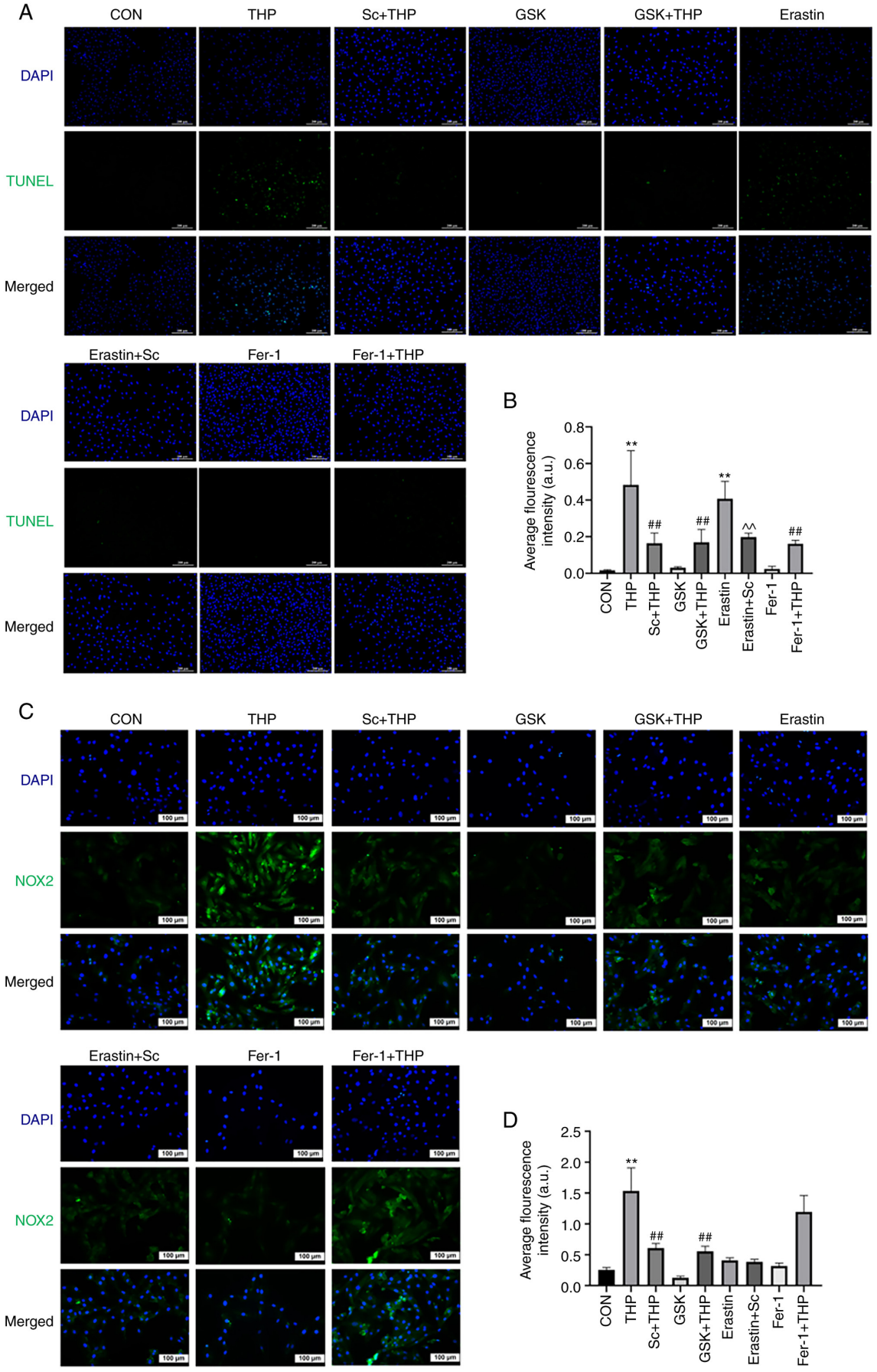

Figure 6. Effects of Sc, THP, GSK, Fer-1, and erastin on the apoptosis of H9c2 cardiomyocytes and the expression of NOX2. (A) TUNEL assay. (B) Semi-quantitative analysis of the average fluorescence intensity of the results of the TUNEL assay. (C) Immunofluorescence staining of NOX2. (D) Semi-quantitative analysis of the average fluorescence intensity of NOX2. Values are expressed as means ± standard deviation. **P<0.01 vs. CON. $^{\#\#}$P<0.01 vs. THP. $^{\wedge\wedge}$P<0.01 vs. erastin. Sc, scutellarein; THP, pirarubicin; GSK, GSK2795039; Fer-1, ferrostatin-1; NOX2, NADPH oxidase 2; CON, control.

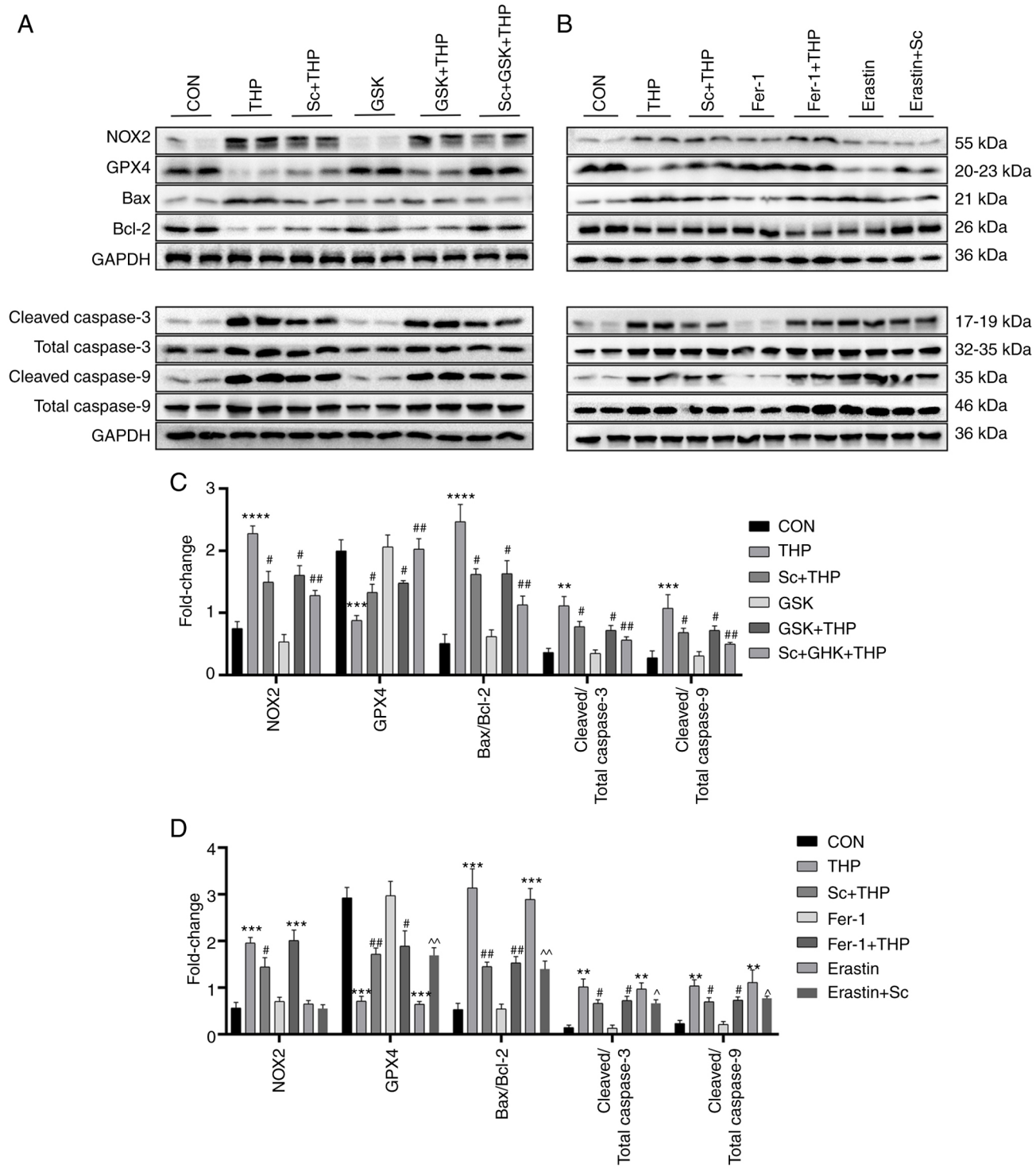

Figure 7. Effects of Sc, THP, GSK, Fer-1, and erastin on oxidative stress, ferroptosis, and apoptosis-related proteins in H9c2 cells. (A and B) Western blots. (C and D) Semi-quantitative analysis of the protein expression of GPX4, NOX2, Bax/Bcl-2, cleaved caspase 3/total caspase 3 and cleaved caspase 9/total caspase 9 in each group. Values are expressed as the means ± standard deviation. **P<0.01, ***P<0.001 and ****P<0.0001 vs. CON. $^{\#}$P<0.05 and $^{\#\#}$P<0.01 vs. THP. $^{\wedge}$P<0.05 and $^{\wedge\wedge}$P<0.01 vs. erastin. Sc, scutellarein; THP, pirarubicin; GSK, GSK2795039; Fer-1, ferrostatin-1; GPX4, glutathione peroxidase 4; NOX2, NADPH oxidase 2.

endogenous accumulation of ROS, which in turn induced lipid peroxidation, ultimately promoting ferroptosis (48,49). Additionally, Fer-1, as a radical-trapping antioxidant, attenuated the accumulation of lipid hydroperoxides via a reduction mechanism, thereby inhibiting ferroptosis (50,51). Notably, in addition to ferroptosis the effects of erastin and Fer-1 were also explored on apoptosis through *in vitro* experiments. The *in vitro* experiments indicated that erastin promoted apoptosis of H9c2 cells, while Fer-1 reduced myocardial cell apoptosis induced by THP. In addition, erastin promoted the expression of apoptosis-related proteins in H9c2 cells (Bax/Bcl-2 and cleaved caspase 3), while Fer-1 improved the aberrant expression of apoptosis-related proteins induced by THP. In addition, research has shown that erastin-induced increases in Bax

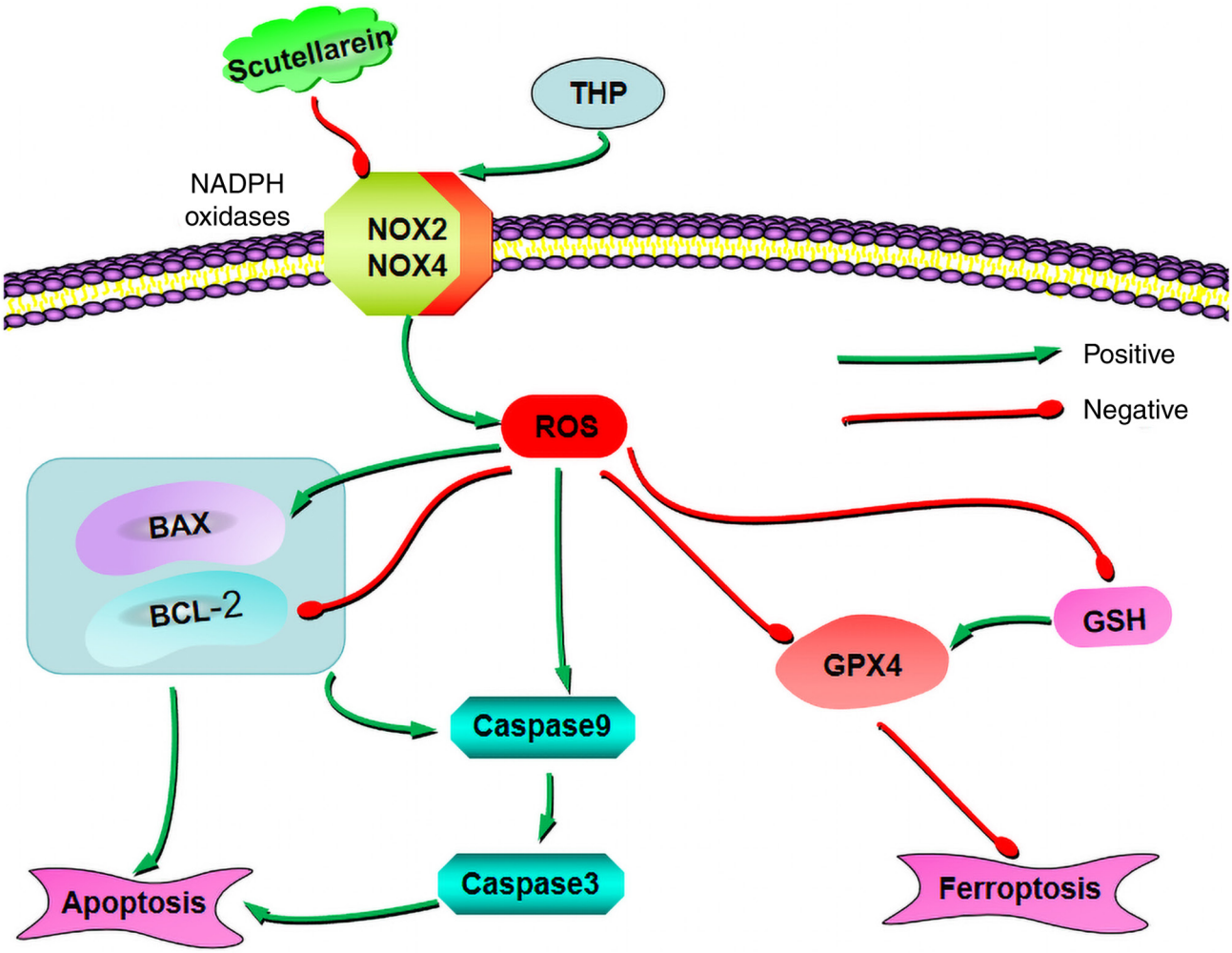

Figure 8. Sc inhibits cell apoptosis and ferroptosis by negatively regulating the oxidative stress axis (NOX2-ROS), thereby improving the cardiotoxicity induced by pirarubicin. NOX2, NADPH oxidase 2; ROS, reactive oxygen species; THP, pirarubicin; NOX4, NADPH oxidase 4; NRF2, erythroid 2-related factor 2; GSH, glutathione; GPX4, glutathione peroxidase 4.

and cytochrome *c* levels were counteracted by ferrostatin-1 pretreatment (52). It was therefore hypothesized that the effects on apoptosis may be associated with the mechanisms of erastin and Fer-1 on regulating ferroptosis via intensifying/inhibiting oxidative stress. Of note, the findings of the present study indicated that the regulation of erastin and Fer-1 for oxidative stress appeared to be independent of NOX2. As aforementioned, oxidative stress is closely associated with apoptosis, and the results revealed that THP downregulated GPX4, thus indicating that THP promoted ferroptosis in myocardial cells. In addition, GSK improved the THP-induced reduction of GPX4 expression, while Sc improved the erastin- and THP-mediated GPX4 downregulation. Furthermore, the combined treatment of myocardial cells with Sc and GSK further improved the THP-mediated reduction of GPX4 expression. The aforementioned findings indicated that regulation of oxidative stress improved the THP-induced ferroptosis in myocardial cells.

The toxic effect of anthracycline drugs on myocardium cannot be ignored, since it is a major public health problem that needs to be urgently solved. Herein, *in vivo* studies demonstrated that CTP was closely associated with oxidative stress, apoptosis and ferroptosis. Therefore, improving CTP via regulation of oxidative stress to inhibit myocardial cell apoptosis and ferroptosis appears to be a feasible strategy. Further experiments verified that food therapy with Sc inhibited cardiomyocyte apoptosis and ferroptosis via regulation of oxidative stress, thereby improving CTP. The aforementioned findings may provide novel insights into the clinical application of Sc and a significant theoretical basis for the implementation of Sc or even all anthracycline antineoplastic drugs in preventing and treating THP-induced cardiotoxicity.

However, the present study has some limitations. Although the current study investigated the protective effect of Sc on THP-induced myocardial injury and its association with oxidative stress, apoptosis and ferroptosis based on existing literature, its specific underlying mechanism remains unclear. In addition, the *in vivo* molecular mechanism underlying the protective effect of Sc on CTP was not explored. Furthermore, clinical trials on the effectiveness of Sc are still lacking. Therefore, further studies and clinical trials on this subject should be carried out in the future.

In conclusion, the present study indicated that Sc had antioxidant, anti-apoptotic, and anti-ferroptosis effects in CTP. In addition, the results suggested that Sc could further inhibit cell apoptosis and ferroptosis via negatively regulating the oxidative stress-related axis, NOX2/ROS, thereby improving the THP-induced cardiotoxicity (Fig. 8).

Acknowledgements

Not applicable.

Funding

This study was supported by the National Key R&D Program of China (grant nos. 2018YFC1311400 and 2018YFC1311404).

Availability of data and materials

The data generated in the present study are not publicly available due the fact that elements of the current basic and clinical research remain uncompleted and ongoing, and as a patent application will be filed. However, data may be requested from the corresponding author.

Authors' contributions

YL and FT confirm the authenticity of all the raw data. YL and FT performed the experiments. HT and PP analyzed and interpreted the data. QH and LD verified the results. YL and FT wrote the manuscript. QH and LD contributed to the conception, design and supervision of the study. All authors reviewed and approved the final version of the manuscript.

Ethics approval and consent to participate

This study was approved by the Animal Ethics Committee of the First Affiliated Hospital of Chongqing Medical University (approval no. IACUC-CQMU-2022-0127, Chongqing, China).

Patient consent for publication

Not applicable.

Competing interests

The authors declare that they have no competing interests.

References

1. Mullard A: Addressing cancer's grand challenges. Nat Rev Drug Discov 19: 825-826, 2020.
2. Hait WN: Anticancer drug development: The grand challenges. Nat Rev Drug Discov 9: 253-254, 2010.
3. von Minckwitz G and Loibl S: Evolution of adjuvant chemotherapy for breast cancer. Lancet 385: 1812-1814, 2015.
4. Shen SJ and Liu CM: Chemotherapy for early-stage breast cancer: The more the better? Lancet 401: 1243-1245, 2023.
5. Gabizon AA, Patil Y and La-Beck NM: New insights and evolving role of pegylated liposomal doxorubicin in cancer therapy. Drug Resist Updat 29: 90-106, 2016.
6. Pugazhendhi A, Edison TNJI, Velmurugan BK, Jacob JA and Karuppusamy I: Toxicity of Doxorubicin (Dox) to different experimental organ systems. Life Sci 200: 26-30, 2018.
7. Yu J, Wang C, Kong Q, Wu X, Lu JJ and Chen X: Recent progress in doxorubicin-induced cardiotoxicity and protective potential of natural products. Phytomedicine 40: 125-139, 2018.
8. Kong CY, Guo Z, Song P, Zhang X, Yuan YP, Teng T, Yan L and Tang QZ: Underlying the mechanisms of doxorubicin-induced acute cardiotoxicity: Oxidative stress and cell death. Int J Biol Sci 18: 760-770, 2022.
9. Tocchetti CG, Carpi A, Coppola C, Quintavalle C, Rea D, Campesan M, Arcari A, Piscopo G, Cipresso C, Monti MG, *et al*: Ranolazine protects from doxorubicin-induced oxidative stress and cardiac dysfunction. Eur J Heart Fail 16: 358-366, 2014.
10. Zhao L, Tao X, Qi Y, Xu L, Yin L and Peng J: Protective effect of dioscin against doxorubicin-induced cardiotoxicity via adjusting microRNA-140-5p-mediated myocardial oxidative stress. Redox Biol 16: 189-198, 2018.
11. McLaughlin D, Zhao Y, O'Neill KM, Edgar KS, Dunne PD, Kearney AM, Grieve DJ and McDermott BJ: Signalling mechanisms underlying doxorubicin and Nox2 NADPH oxidase-induced cardiomyopathy: Involvement of mitofusin-2. Br J Pharmacol 174: 3677-3695, 2017.
12. Li Q, Qin M, Tan Q, Li T, Gu Z, Huang P and Ren L: MicroRNA-129-1-3p protects cardiomyocytes from pirarubicin-induced apoptosis by down-regulating the GRIN2D-mediated Ca^{2+} signalling pathway. J Cell Mol Med 24: 2260-2271, 2020.
13. Han D, Wang Y, Wang Y, Dai X, Zhou T, Chen J, Tao B, Zhang J and Cao F: The tumor-suppressive human circular RNA CircITCH sponges miR-330-5p to ameliorate doxorubicin-induced cardiotoxicity through upregulating SIRT6, survivin, and SERCA2a. Circ Res 127: e108-e125, 2020.
14. Chen YH, Chen ZW, Li HM, Yan XF and Feng B: AGE/RAGE-Induced EMP release via the NOX-Derived ROS pathway. J Diabetes Res 2018: 6823058, 2018.
15. Zhang J, Wang X, Vikash V, Ye Q, Wu D, Liu Y and Dong W: ROS and ROS-Mediated cellular signaling. Oxid Med Cell Longev 2016: 4350965, 2016.
16. Drummond GR and Sobey CG: Endothelial NADPH oxidases: Which NOX to target in vascular disease? Trends Endocrinol Metab 25: 452-463, 2014.
17. Prosser BL, Ward CW and Lederer WJ: X-ROS signaling: Rapid mechano-chemo transduction in heart. Science 333: 1440-1445, 2011.
18. Orrenius S, Gogvadze V and Zhivotovsky B: Mitochondrial oxidative stress: Implications for cell death. Annu Rev Pharmacol Toxicol 47: 143-183, 2007.
19. Stockwell BR: Ferroptosis turns 10: Emerging mechanisms, physiological functions, and therapeutic applications. Cell 185: 2401-2421, 2022.
20. Spiegel M, Marino T, Prejanò M and Russo N: On the scavenging ability of scutellarein against the OOH radical in water and Lipid-like environments: A Theoretical study. Antioxidants (Basel) 11: 224, 2022.
21. Lin Y, Lin Y, Ren N, Li S, Chen M and Pu P: Novel anti-obesity effect of scutellarein and potential underlying mechanism of actions. Biomed Pharmacother 117: 109042, 2019.
22. Chagas MDSS, Behrens MD, Moragas-Tellis CJ, Penedo GXM, Silva AR and Gonçalves-de-Albuquerque CF: Flavonols and flavones as potential anti-inflammatory, antioxidant, and antibacterial compounds. Oxid Med Cell Longev 2022: 9966750, 2022.
23. Gao L, Tang H, Zeng Q, Tang T, Chen M and Pu P: The anti-insulin resistance effect of scutellarin may be related to antioxidant stress and AMPKα activation in diabetic mice. Obes Res Clin Pract 14: 368-374, 2020.
24. Mei X, Zhang T, Ouyang H, Lu B, Wang Z and Ji L: Scutellarin alleviates blood-retina-barrier oxidative stress injury initiated by activated microglia cells during the development of diabetic retinopathy. Biochem Pharmacol 159: 82-95, 2019.
25. Shi H, Tang H, Ai W, Zeng Q, Yang H, Zhu F, Wei Y, Feng R, Wen L, Pu P and He Q: Schisandrin B antagonizes cardiotoxicity induced by pirarubicin by inhibiting mitochondrial permeability transition pore (mPTP) opening and decreasing cardiomyocyte apoptosis. Front Pharmacol 12: 733805, 2021.
26. Chai Y, Cao Z, Yu R, Liu Y, Yuan D and Lei L: Dexmedetomidine attenuates LPS-Induced Monocyte-Endothelial adherence via inhibiting Cx43/PKC-α/NOX2/ROS signaling pathway in monocytes. Oxid Med Cell Longev 2020: 2930463, 2020.
27. Zhang H, Wang Z, Liu Z, Du K and Lu X: Protective effects of dexazoxane on rat ferroptosis in Doxorubicin-Induced cardiomyopathy through regulating HMGB1. Front Cardiovasc Med 8: 685434, 2021.
28. Li S, Lei Z, Yang X, Zhao M, Hou Y, Wang D, Tang S, Li J and Yu J: Propofol protects myocardium from ischemia/reperfusion injury by inhibiting ferroptosis through the AKT/p53 signaling pathway. Front Pharmacol 13: 841410, 2022.
29. Lim GB: Circular RNA prevents doxorubicin-induced cardiotoxicity. Nat Rev Cardiol 19: 574, 2022.

30. Gianni L, Herman EH, Lipshultz SE, Minotti G, Sarvazyan N and Sawyer DB: Anthracycline cardiotoxicity: From bench to bedside. J Clin Oncol 26: 3777-3784, 2008.
31. Han XZ, Gao S, Cheng YN, Sun YZ, Liu W, Tang LL and Ren DM: Protective effect of naringenin-7-O-glucoside against oxidative stress induced by doxorubicin in H9c2 cardiomyocytes. Biosci Trends 6: 19-25, 2012.
32. Alanazi AM, Fadda L, Alhusaini A, Ahmad R, Hasan IH and Mahmoud AM: Liposomal resveratrol and/or carvedilol attenuate doxorubicin-induced cardiotoxicity by modulating inflammation, oxidative stress and S100A1 in rats. Antioxidants (Basel) 9: 159, 2020.
33. Rosca MG and Hoppel CL: Mitochondria in heart failure. Cardiovasc Res 88: 40-50, 2010.
34. Hausenloy DJ and Ruiz-Meana M: Not just the powerhouse of the cell: Emerging roles for mitochondria in the heart. Cardiovasc Res 88: 5-6, 2010.
35. ChenYR and Zweier JL: Cardiac mitochondria and reactive oxygen species generation. Circ Res 114: 524-537, 2014.
36. Bedard K and Krause KH: The NOX family of ROS-generating NADPH oxidases: physiology and pathophysiology. Physiol Rev 87: 245-313, 2007.
37. Li D, Yang Y, Wang S, He X, Liu M, Bai B, Tian C, Sun R, Yu T and Chu X: Role of acetylation in doxorubicin-induced cardiotoxicity. Redox Biol 46: 102089, 2021.
38. D'Autreaux B and Toledano MB: ROS as signalling molecules: Mechanisms that generate specificity in ROS homeostasis. Nat Rev Mol Cell Biol 8: 813-824, 2007.
39. Stockwell BR: A powerful cell-protection system prevents cell death by ferroptosis. Nature 575: 597-598, 2019.
40. Tang D, Chen X, Kang R and Kroemer G: Ferroptosis: Molecular mechanisms and health implications. Cell Res 31: 107-125, 2021.
41. Park MW, Cha HW, Kim J, Kim JH, Yang H, Yoon S, Boonpraman N, Yi SS, Yoo ID and Moon JS: NOX4 promotes ferroptosis of astrocytes by oxidative stress-induced lipid peroxidation via the impairment of mitochondrial metabolism in Alzheimer's diseases. Redox Biol 41: 101947, 2021.
42. Bersuker K, Hendricks JM, Li Z, Magtanong L, Ford B, Tang PH, Roberts MA, Tong B, Maimone TJ, Zoncu R, *et al*: The CoQ oxidoreductase FSP1 acts parallel to GPX4 to inhibit ferroptosis. Nature 575: 688-692, 2019.
43. Jiang X, Stockwell BR and Conrad M: Ferroptosis: Mechanisms, biology and role in disease. Nat Rev Mol Cell Biol 22: 266-282, 2021.
44. Conrad M and Pratt DA: The chemical basis of ferroptosis. Nat Chem Biol 15: 1137-1147, 2019.
45. Liu Z, Zhou Z, Ai P, Zhang C, Chen J and Wang Y: Astragaloside IV attenuates ferroptosis after subarachnoid hemorrhage via Nrf2/HO-1 signaling pathway. Front Pharmacol 13: 924826, 2022.
46. Dixon SJ, Lemberg KM, Lamprecht MR, Skouta R, Zaitsev EM, Gleason CE, Patel DN, Bauer AJ, Cantley AM, Yang WS, *et al*: Ferroptosis: An iron-dependent form of nonapoptotic cell death. Cell 149: 1060-1072, 2012.
47. Yan R, Xie E, Li Y, Li J, Zhang Y, Chi X, Hu X, Xu L, Hou T, Stockwell BR, *et al*: The structure of erastin-bound xCT-4F2hc complex reveals molecular mechanisms underlying erastin-induced ferroptosis. Cell Res 32: 687-690, 2022.
48. Gan B: How erastin assassinates cells by ferroptosis revealed. Protein Cell 14: 84-86, 2023.
49. Yang Y, Luo M, Zhang K, Zhang J, Gao T, Connell DO, Yao F, Mu C, Cai B, Shang Y and Chen W: Nedd4 ubiquitylates VDAC2/3 to suppress erastin-induced ferroptosis in melanoma. Nat Commun 11: 433, 2020.
50. Zilka O, Shah R, Li B, Friedmann Angeli JP, Griesser M, Conrad M and Pratt DA: On the mechanism of cytoprotection by Ferrostatin-1 and Liproxstatin-1 and the role of lipid peroxidation in ferroptotic cell death. ACS Cent Sci 3: 232-243, 2017.
51. Miotto G, Rossetto M, Di Paolo ML, Orian L, Venerando R, Roveri A, Vučković AM, Bosello Travain V, Zaccarin M, Zennaro L, *et al*: Insight into the mechanism of ferroptosis inhibition by ferrostatin-1. Redox Biol 28: 101328, 2020.
52. Park JS, Kim DH, Choi HI, Kim CS, Bae EH, Ma SK and Kim SW: 3-Carboxy-4-methyl-5-propyl-2-furanpropanoic acid (CMPF) induces cell death through ferroptosis and acts as a trigger of apoptosis in kidney cells. Cell Death Dis 14: 78, 2023.